Location and Aggregation of the Spin-Labeled Peptide Trichogin GA IV in a Phospholipid Membrane as Revealed by Pulsed EPR

E. S. Salnikov,* D. A. Erilov,* A. D. Milov,* Yu. D. Tsvetkov,* C. Peggion,† F. Formaggio,† C. Toniolo,† J. Raap,‡ and S. A. Dzuba*

*Institute of Chemical Kinetics and Combustion, Academy of Sciences, 630090 Novosibirsk, Russia; †Department of Chemistry, University of Padova, 35131 Padua, Italy; and ‡Leiden Institute of Chemistry, Gorlaeus Laboratories, University of Leiden, 2300 RA Leiden, The Netherlands

ABSTRACT The lipopeptaibol trichogin GA IV is a 10 amino acid-long residue and α-aminoisobutyric acid-rich antibiotic peptide of fungal origin. TOAC (2,2,6,6-tetramethylpiperidine-1-oxyl-4-amino-4-carboxylic acid) spin-labeled analogs of this membrane active peptide were investigated in hydrated bilayers of dipalmitoylphosphatidylcholine by electron spin echo envelope modulation (ESEEM) spectroscopy and pulsed electron-electron double resonance (PELDOR). Since, the ESEEM of the spin label appears to be strongly dependent on the presence of water molecules penetrated into the membrane, this phenomenon was used to study the location of this peptide in the membrane. This was achieved by comparing the ESEEM spectra for peptides labeled at different positions along the amino acid sequence with spectra known for lipids with spin labels at different positions along the hydrocarbon chain. To increase the ESEEM amplitude and to distinguish the hydrogen nuclei of water from lipid protons, membranes were hydrated with deuterated water. The PELDOR spectroscopy technique was chosen to study peptide aggregation and to determine the mutual distance distribution of the spin-labeled peptides in the membrane. The location of the peptide in the membrane and its aggregation state were found to be dependent on the peptide concentration. At a low peptide/lipid molar ratio (less than 1:100) the nonaggregated peptide chain of the trichogin molecules lie parallel to the membrane surface, with TOAC at the 4th residue located near the 9th–11th carbon positions of the *sn-2* lipid chain. Increasing this ratio up to 1:20 leads to a change in peptide orientation, with the N-terminus of the peptide buried deeper into membrane. Under these conditions peptide aggregates are formed with a mean aggregate number of about $N = 2$. The aggregates are further characterized by a broad range of intermolecular distances (1.5–4 nm) between the labels at the N-terminal residues. The major population exhibits a distance of ~2.5 nm, which is of the same order as the length of the helical peptide. We suggest that the constituting monomers of the dimer are antiparallel oriented.

INTRODUCTION

Trichogin GA IV, isolated from the mold *Trichoderma longibrachiatum* (1), belongs to the class of peptaibols characterized by a high percentage of α-aminoisobutyric acid (Aib) residues and an 1,2-amino alcohol at the C-terminus (2). The primary structure of this peptaibol is unique due to its lipophilic *n*-octanoyl group at the N-terminus instead of the acetyl group present in most of the other members of this class. Despite the short length of its main chain (10 amino acid residues), trichogin GA IV exhibits remarkable membrane-modifying properties (for recent review articles, see Rebuffat et al. (3), Toniolo et al. (4), and Peggion et al. (5)).

To elucidate the mechanism by which this short peptide changes the membrane permeability, detailed information is needed on where it is located in the membrane. Orientation and immersion depth of trichogin GA IV were studied using different experimental methods. Previously, hyperfine interaction (hfi) constants of 2,2,6,6-tetramethylpiperidine-1-oxyl-4-amino-4-carboxylic acid (TOAC) spin-labeled trichogin analogs in membranes of phosphatidylcholine liposomes were analyzed as a function of environmental polarity (6). Trichogin was found to be oriented parallel to the membrane surface with the hydrophobic side chains facing toward the membrane interior. However, this approach (3) is based on the questionable procedure of deriving hfi constants, which are not only related to the perpendicular orientation constant, $A_\perp$, but also depend on molecular motion. Another approach to assess the degree of insertion of the peptide in the membrane was based on the quenching of fluorescence of 4,4-difluoro-4-bora-3a,4a-diaza-S-indacene (BODIPY)-labeled lipids by nitroxide spin labels located at different positions of the peptide chain (7,8). However, as this bulky fluorophoric group attached to phospholipid has a clear tendency to migrate from the hydrocarbon core to the polar headgroup region of the bilayer (8), the validity of this method is even less reliable.

Recently, Mazzuca et al. (9) employed fluorescence quenching measurements to investigate the membrane-bound state of trichogin. It was found to depend on the peptide concentration. At low peptide/lipid (P/L) ratios the trichogin molecules are located close to the polar region of lipid headgroups. By increasing the peptide concentration until membrane leakage takes place, a cooperative transition occurs and a significant fraction of the peptide becomes buried deeper into the bilayer.

Submitted October 12, 2005, and accepted for publication April 25, 2006.

Address reprint requests to Dr. J. Raap, Leiden Institute of Chemistry, Gorlaeus Laboratories, University of Leiden, 2300RA Leiden, The Netherlands. Fax: 31-715274537; E-mail: j.raap@chem.leidenuniv.nl.

0006-3495/06/08/1532/09 $2.00

doi: 10.1529/biophysj.105.075887

In this work, we have chosen the electron spin echo envelope modulation (ESEEM) technique (10) to study the orientation and immersion depth of trichogin GA IV molecules in the membrane. The phenomenon of this pulsed electron paramagnetic resonance (EPR) technique originates from the dependence of anisotropic hfi constants of nitroxide spins with nearby protons of water molecules. Since water molecules are capable of penetrating into the hydrophobic core of the membrane, the amplitude of the ESEEM spectrum of a spin-labeled peptide would provide information on the depth of its label position. Comparison of these data obtained for peptides spin-labeled at different positions will allow us to determine the peptide orientation. Overall, this approach may give precise information on the location of the peptide within the membrane. We used deuterated water (D_2O) to distinguish hydrogen atoms of water from those of lipid molecules and to increase the amplitude of the ESEEM that is known to be much larger for deuterons at the x-band. An analogous approach was employed previously (11), wherein the location of a doxylstearic acid spin probe in lipid bilayers was studied by ESEEM induced by its interaction with ^{31}P of phospholipids.

To provide complementary information about the bound state of trichogin GA IV in the lipid bilayer, the pulsed electron-electron double resonance (PELDOR, sometimes called DEER) technique (12,13) was employed. This technique makes it possible to measure the dipole-dipole interaction between spins and to provide information about the aggregation state of this amphipathic peptide. In previous attempts we failed to detect aggregates of trichogin in dipalmitoylphosphatidylcholine (DPPC) membranes at a P/L molar ratio up to 1:125 (14).

In this work, we describe the peculiarities of trichogin GA IV analogs spin labeled with TOAC in the presence of multilamellar DPPC membranes (frozen at 77 K) over a broader range of P/L ratios. The primary structures of trichogin GA IV and its analogs are listed below. In all these peptide analogs, the C-terminal leucinol (Lol) is replaced by its synthetic precursor L-leucine methyl ester (Leu-OMe). In three analogs the N-terminal *n*-octanoyl (*n*Oct) group is substituted by the 9-fluorenylmethyloxycarbonyl (Fmoc) group. It is known that these replacements do not alter the three-dimensional structural properties nor the membrane activity of trichogin (1,4,5,15,16).

MATERIALS AND METHODS

DPPC and D_2O were obtained from Sigma-Aldrich (Zwijndrecht, The Netherlands). The synthesis and characterization of the spin-labeled trichogin GA IV analogs FTOAC1, FTOAC4, FTOAC8, *n*Oct-TOAC1, and *n*Oct-TOAC4 were already described (6). For the preparation of a 10 mM D_2O phosphate buffer solution (PBS) at pH 7.4, reagent grade salts were obtained from Sigma-Aldrich. All commercial materials were used without further purification.

Sample preparation

DPPC and the spin-labeled peptide were codissolved in chloroform solution. The solvent was first evaporated with a nitrogen gas stream. Then, residual traces of solvent were removed by drying the mixture under vacuum for at least 3 h. The mixture was dispersed in PBS at a concentration of ~100 mg/ml by vortex mixing with heating to 55°C, i.e., above the phase transition temperature of DPPC. The hydrated lipid bilayers were finally transferred to a glass EPR tube and concentrated by pelleting in a benchtop centrifuge. Then, the excess buffer was removed. The final water concentration was ~30% w/w. Before measuring, samples were incubated for 24 h at 10°C. All measurements were performed at the liquid nitrogen temperature. Samples were cooled optionally by shock freezing at the liquid nitrogen temperature or slowly at ~3°C per min.

Pulsed EPR spectroscopy

ESEEM experiments were performed on a Bruker ESP 380E pulse x-band EPR spectrometer. A homemade rectangular resonator (H_{012} mode) was used, with a quartz Dewar containing liquid nitrogen. The resonator was overcoupled to obtain a dead time of 100 ns. Three pulse-stimulated echo ($\pi/2$-τ-$\pi/2$-T-$\pi/2$-τ-echo) decays were obtained by using microwave pulse widths of 16 ns, with the microwave power adjusted accordingly. The time delay T between the second and the third pulses was incremented while maintaining the separation τ between the first and the second pulses constant at 200 ns to maximize deuterium modulation. A four-step phase-cycling program was employed to eliminate unwanted echoes.

The data were treated as follows (11,17): 1), the experimental echo decay was approximated with a biexponential function (see Fig. 1, *a* and *c*); 2), the data were then divided by this function, so that only oscillations around the unity remained (Fig. 1, *b* and *d*); 3), the unit level was subtracted from the signal; 4), the array of ESEEM data was zero filled to increase the total number of points up to 4096; and 5), a numerical Fourier transformation was performed. Note that when different samples are compared, such a procedure allows one to obtain the relative contribution of the modulated electron spin echo signal (the unity in step (2) represents a nonmodulated contribution) from which quantitative information about the relative positions of nearby nuclei can be provided.

PELDOR studies were carried out using a PELDOR spectrometer with a bimodal cavity and two independent pulse sources as described in Milov et al. (12) and Milov et al. (13). The position of the pumping pulse

*n*Oct-Aib^{1}-Gly-Leu-Aib^{4}-Gly-Gly-Leu-Aib^{8}-Gly-Ile-Lol (trichogin GA IV)

*n*Oct-**TOAC**^{1}-Gly-Leu-Aib^{4}-Gly-Gly-Leu-Aib^{8}-Gly-Ile-Leu-OMe (*n*Oct-TOAC1)

nOct-Aib^{1}-Gly-Leu-**TOAC**^{4}-Gly-Gly-Leu-Aib^{8}-Gly-Ile-Leu-OMe (*n*Oct-TOAC4)

Fmoc-**TOAC**^{1}-Gly-Leu-Aib^{4}-Gly-Gly-Leu-Aib^{8}-Gly-Ile-Leu-OMe (FTOAC1)

Fmoc-Aib^{1}-Gly-Leu-**TOAC**^{4}-Gly-Gly-Leu-Aib^{8}-Gly-Ile-Leu-OMe (FTOAC4)

Fmoc-Aib^{1}-Gly-Leu-Aib^{4}-Gly-Gly-Leu-**TOAC**^{8}-Gly-Ile-Leu-OMe (FTOAC8)

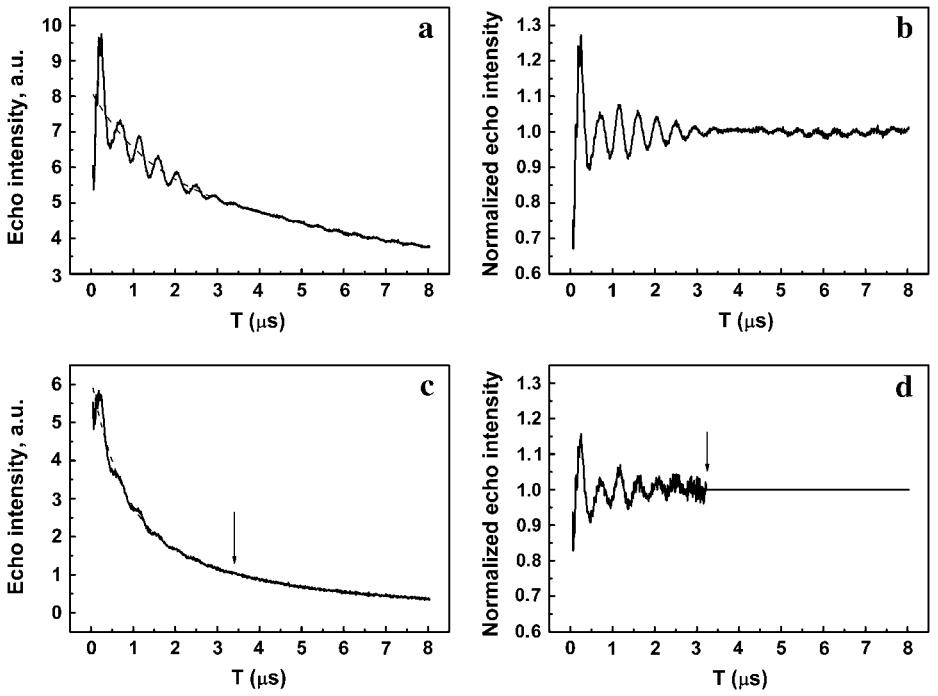

FIGURE 1 Experimental ESEEM traces obtained for the spin-labeled peptide FTOAC1 in a DPPC membrane, hydrated in D_2O, for P/L molar ratios of 1:250 (*a*, *b*) and 1:20 (*c*, *d*). Original data, given in (*a*) and (*c*), are approximated by a biexponential decay (*dashed lines*). Data in (*b*) and (*d*) are the result of dividing the original data by these decay functions. The arrow marks the point of data truncation to reduce the level of noise.

corresponded to the maximum amplitude in the electron spin resonance (ESR) spectrum. The frequency difference between two microwave sources was 65 MHz (so that the echo was formed by spins corresponding to the low-field shoulder of the nitroxide EPR spectrum). The pumping pulse is switched on between the first and second pulses and is delayed by time T after the first pulse. The PELDOR signal is the signal of the spin echo, $V(T)$. Durations of the first and second pulses forming the spin echo signal were 40 and 70 ns, respectively. The duration of the pumping pulse was 30 ns. Its amplitude was selected to provide the probability to induce a flip of the spins, p_b near 0.1, which is suitable for measurements of aggregation (see below). For a model biradical system the experimental value of p_b was found to be 0.09 ± 0.01.

The molecular model shown (see Fig. 8) was constructed by using the program WebLab Viewer Pro 4.0 (Molecular Simulations, Cambridge, MA). The three-dimensional structure of the peptide backbone of trichogin GA IV, taken from its x-ray diffraction analysis (18), is similar to the crystal structure of double spin-labeled *n*Oct-TOAC4,8 (19,20).

RESULTS

ESEEM data

An example of the experimental time-domain ESEEM data is shown in Fig. 1 for FTOAC1 bound to DPPC bilayers hydrated in D_2O, at two different peptide concentrations. Fig. 1, *a* and *c*, presents original data which were approximated by exponential decays. Fig. 1, *b* and *d*, shows the result of their division by these decay functions. It is evident that at high concentration the decay is remarkably faster (compare Fig. 1, *a* and *c*), which may be readily explained by the concentration dependence of transverse relaxation. Because of the fast decay at high concentration and the consequential increase of noise at large T, data in Fig. 1 *d* were truncated at $T > 3.5$ μs. Within the experimental accuracy, the results were found to be independent on how the sample was cooled (see Materials and Methods).

Fig. 2 shows the modulus Fourier transform spectra for three samples (FTOAC1, FTOAC4, and FTOAC8) at a P/L molar ratio of 1:250. One can see a narrow doublet at frequency 2.2 MHz, overlapped by a broader line. Since 2.2 MHz is the Larmor frequency of the deuterium nuclei in the magnetic field employed, both of these lines may be readily attributed to the anisotropic hfi between the unpaired electron of the nitroxide label and the deuterium nuclei of water molecules. The narrow doublet, according to the comprehensive analysis performed in Erilov et al. (17), may be assigned to free water present at the hydrocarbon chain region of the membrane, whereas the broad line indicates water molecules bound to the N-O group of the spin label. The doublet is caused by the quadrupolar splitting for the deuterium spin with $I = 1$.

The highest amplitude of the deuterium line is observed for the sample containing the membrane-bound trichogin analog labeled at the N-terminus (FTOAC1). Compared to FTOAC1, the sample with the analog labeled near the C-terminus (FTOAC8) shows a decreased amplitude (by ~20%) for the deuterium line, whereas in the case of the peptide labeled in the middle of the peptide chain (FTOAC4) the amplitude of the deuterium line is most strongly decreased by ~60%.

Fig. 3, *a* and *b*, shows the modulus Fourier transform spectra for membrane-bound samples of *n*Oct-TOAC1 and FTOAC1 at a P/L molar ratio of 1:250 (note that the spectrum shown in Fig. 3 *a* coincides with that of Fig. 2 *a*). It is clear that both spectra are nearly the same. Fig. 3 *c* shows data adapted from Erilov et al. (17) presenting ESEEM

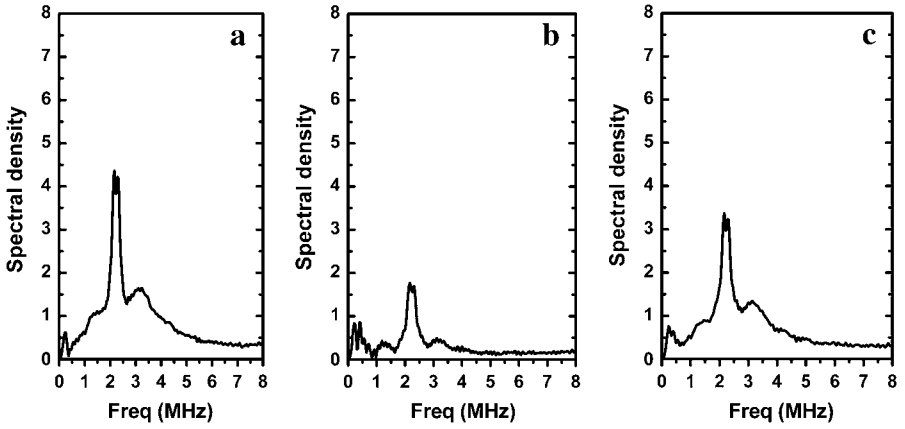

FIGURE 2 Modulus Fourier-transform ESEEM spectra obtained for a P/L molar ratio of 1:250. (*a*) FTOAC1, (*b*) FTOAC4, and (*c*) FTOAC8.

amplitudes of nitroxide labels at different positions of the *sn*-2 fatty acyl side chain of DPPC lipid molecules which are incorporated into unlabeled DPPC membranes. As the membrane was obtained under the same experimental conditions as those employed in this work, the data in Fig. 3 *c* may serve as a calibration curve for determining the membrane insertion of nitroxide-labeled trichogin molecules. Fig. 4 shows the modulus Fourier transform spectra for three samples, with FTOAC1, FTOAC4, and FTOAC8 analogs at a P/L molar ratio of 1:20. In comparison with the data obtained at lower peptide concentration (Fig. 2), a remarkable decreased line amplitude is observed for FTOAC1, whereas those for FTOAC4 and FTOAC8 decrease only slightly. The unresolved doublet at frequency 2.2 MHz may be explained by a broadening due to fast relaxation induced by electron-electron spin-spin interactions at a high spin-label concentration. Note that this broadening may result also in a slight decrease of intensity, which should be taken into account when comparing with samples of low spin concentration.

PELDOR data

In Fig. 5 the PELDOR signal $V(T)$ is plotted for DPPC bilayers containing FTOAC1 at P/L molar ratios of 1:20 and 1:30, respectively. These traces are normalized by dividing the signal value V_0 in the absence of the pumping pulse. In cases where peptides form aggregates, the contributions from intra- and interaggregate interactions are assumed to be independent, and $V(T)$ may be written as a multiplication, $V(T) = V_{\mathrm{INTRA}}(T)V_{\mathrm{INTER}}(T)$, where $V_{\mathrm{INTRA}}(T)$ and $V_{\mathrm{INTER}}(T)$ are the PELDOR signals arising from intra- and intermolecular interactions between spin labels, respectively (13,14). According to Milov et al. (14), it can be assumed that $V_{\mathrm{INTER}}(T)$ depends on concentration C as follows:

$$V_{\mathrm{INTER}}(T) = \exp(-p_{\mathrm{b}}Cf(T)), \tag{1}$$

where $f(T)$ is a function of time, T. Then, using two experimental dependencies, $V_1(T)$ and $V_2(T)$, for two different spin label concentrations, C_1 and C_2,

$$\ln(V_2) - \ln(V_1) = p_{\mathrm{b}}(C_1 - C_2)f(T). \tag{2}$$

The set of data points 3 in Fig. 5 is obtained by subtracting the data of sets 1 and 2. The solid line drawn through this set of points is an approximation by a third-order polynomial function, which is referred to below as function $G(T)$. Since the concentrations C_1 and C_2, as well as p_{b}, are known with a limited accuracy, we used the relation Eq. 3 to obtain $V_{\mathrm{INTRA}}(T)$.

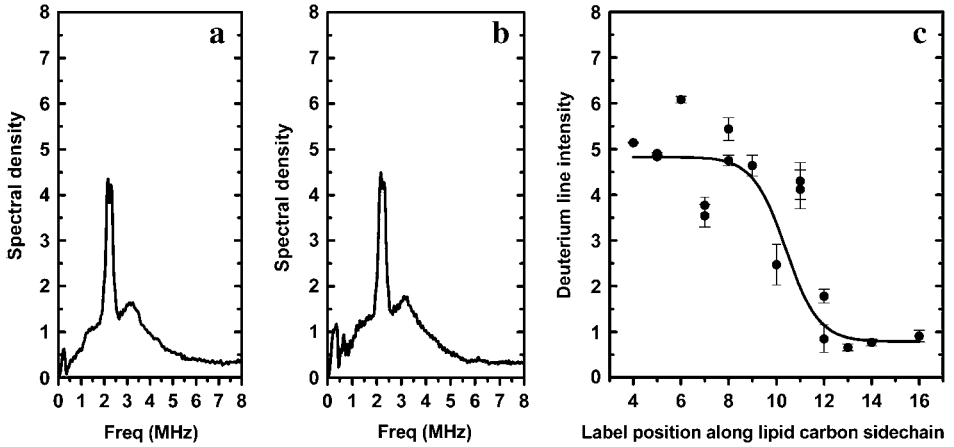

FIGURE 3 Modulus Fourier-transform ESEEM spectra recorded by using a sample at a P/L molar ratio of 1:250 for (*a*) FTOAC1 (the spectrum is the same as shown in Fig. 2 *a*) and (*b*) *n*Oct-TOAC1. (*c*) Calibration curve representing ESEEM amplitudes for lipids spin-labeled at different positions along the hydrocarbon side chain (adapted from Erilov et al. (17)).

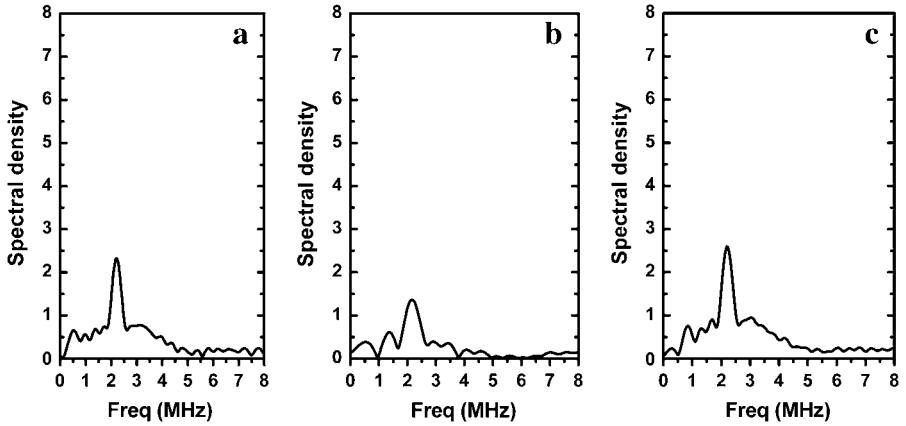

FIGURE 4 Modulus Fourier-transform ESEEM spectra for a P/L molar ratio of 1:20 for (*a*) FTOAC1, (*b*) FTOAC4, and (*c*) FTOAC8.

$$\ln V_{\mathrm{INTRA}} = \ln V_1 + k\frac{C_1}{C_2 - C_1}G(t). \qquad (3)$$

The coefficient k (which is close to unity) was taken to make the values $d(\ln(V))/dT$ and $d(k\ln(V_{\mathrm{INTER}}))/dT$ coincide with each other in the region of large T values. This method, which allows one to determine $V_{\mathrm{INTRA}}(T)$ more accurately, is applicable if it tends to a limit value at large T. The results obtained are presented in Fig. 6 (the oscillations of the data points shown at $T > 200$ ns are noise).

DISCUSSION

Trichogin orientation and location in the membrane from ESEEM data

Water concentration profiles obtained for the same model membranes as those used in this work were previously reported in Erilov et al. (17), using phospholipids systematically labeled at different locations of the *sn*-2 hydrocarbon chain of the lipid fatty acyl group. Also the experimental ESEEM data were treated in the same way. In this early work the line shapes of the frequency peaks were found similar to those obtained in this study (Figs. 2–4). Therefore, one may directly compare the peak amplitudes found for the same frequency domain in these two different studies. If it is assumed that trichogin doesn't alter the water concentration profile in the membrane, then the comparison with data from Erilov et al. (17) (see Fig. 3 *c*) will readily provide information on the depth of peptide immersion. Fig. 3 *c* shows that the peak amplitude is nearly independent on the label positions of the hydrocarbon chain between the fourth and ninth carbon atoms, thereby forming a plateau with a mean amplitude of ~5 (the value, given in units, scatters between 4 and 6 due to the experimental uncertainty). The amplitude sharply decreases for higher numbers of spin-label positions. Taking that into account, one may readily conclude from the data shown in Fig. 2 that at a P/L molar ratio of 1:250 both spin labels in FTOAC1 and FTOAC8 lie above the 9th–11th positions (closer to the membrane surface), whereas that in FTOAC4 is located below the 11th position (closer to the hydrocarbon core of the membrane).

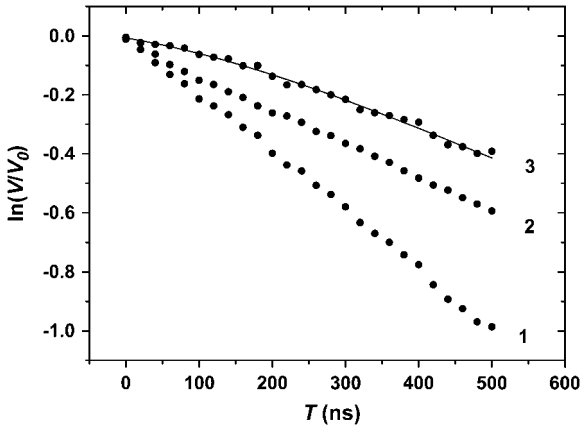

FIGURE 5 PELDOR signal decays for FTOAC1 at P/L molar ratios of 1:20 (data set 1) and 1:30 (set 2). The points of data set 3 are calculated by subtracting those of set 2 from 1. The solid line is an approximation calculated by a third-order polynomial function.

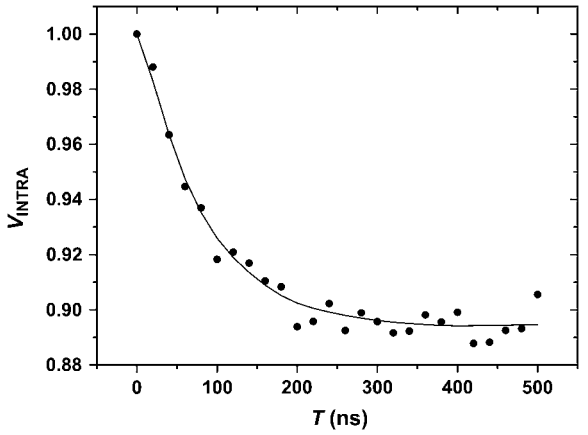

FIGURE 6 Dependence of $V_{\mathrm{INTRA}}(T)$ as obtained from data set 3 in Fig. 5 using relation Eq. 3. The solid line is calculated from relation Eq. 8 (see text).

Interestingly, the ESEEM spectra for FTOAC1 and *n*Oct-TOAC1 are nearly the same (Fig. 3). An analogous result was obtained for FTOAC4 and *n*Oct-TOAC4 (data not shown). Therefore, we conclude that replacement of the *n*Oct-group by Fmoc does not have any effect on the peptide orientation nor on the location in the membrane (at a small P/L molar ratio).

We conclude that at low concentration the peptide chains are located parallel to the membrane surface. Note that in Erilov et al. (17) it was concluded that the density of the lipid chain packing increases below the level of the 11th carbon. Thus, trichogin GA IV is located above this high-density base.

Increasing the relative molar peptide concentration up to a P/L molar ratio of 1:20 leads to a dramatic decrease in the peak intensity of FTOAC1, whereas the spectra of FTOAC4 and FTOAC8 exhibit only a slight decrease of intensities (compare Fig. 2 and Fig. 4). This result suggests that the N-terminus of trichogin is buried at increased concentration. Note that we have no information about a possible change of the peptide secondary structure upon changing the peptide concentration.

Distance distribution function between spin labels from PELDOR data

We define the distance distribution function between spin labels in aggregates as $F(r) = dn(r)/dr$, where $dn(r)$ is the portion of spin labels in the aggregate with a distance in the range between r and $r + dr$. For a pair of two spins separated by a defined distance, r, the PELDOR signal is

$$U(r,T) = 1 - p_b\{1 - f(r,T)\}, \tag{4}$$

where

$$f(r,T) = \left\langle \cos\left[\frac{\gamma^2\hbar}{r^3}(1 - 3\cos^2(\theta))T\right]\right\rangle_\theta .$$

Here, r is the distance between labels, θ is the angle between the vector r and the external direction of the magnetic field, and $\langle \ldots \rangle_\theta$ indicates the θ angle average. We assume below that the spin label pairs are randomly oriented in the aggregates.

For an aggregate consisting of N spin labels while the i^{th} label is participating in the formation of a spin echo, the PELDOR signal is given by the product

$$U_i(T) = \prod_{\substack{j=1\\ j\neq 1}}^{N} U(r_{i,j},T) \approx U_i(T) = 1 - p_b\left\{(N-1) - \sum_{\substack{j=1\\ j\neq 1}}^{N} f(r_{i,j},T)\right\}. \tag{5}$$

If, as in our case, p_b is small enough, i.e., $(N-1)p_b \ll 1$, reasonable N values might be provided. In the case of a continuous distribution of distances between labels in the aggregates, averaging Eq. 6 over all pairs can be presented as

$$U(T) = V_P + (1 - V_P)p_b \int_{r_1}^{r_2} F(r)f(r,T)dr, \tag{6}$$

where $V_P = 1 - (N-1)p_b$. The integration limits r_1 and r_2 in Eq. 7 restrict a physically reasonable range of distances between the spin labels. By division of the interval from r_1 to r_2 into a set of discrete values, r_k, with the difference dr_k and by replacing the integral in Eq. 7 by a sum, we obtain the expression for $U(T)$ for an experimental set of T_s values,

$$U(T_s) = V_P + (1 - V_P)\sum_{k=1}^{m} F(r_k)\left(\int_{r_k}^{r_k + dr_k} f(r,T_s)drdr_k\right), \tag{7}$$

where m is the number of points in the interval between r_1 and r_2. Eq. 8 enables us to obtain the distribution function $F(r_k)$, by comparison of the experimental T-dependencies $V_{INTRA}(T)$ with the calculated $U(T)$. From the mathematical point of view the problem is ill posed. We applied the Tikhonov regularization method (21) for analysis of the PELDOR data by using a homemade program, employing a gradient descending method. For the additional condition $F(r_k) \geq 0$ ($k = 1, \ldots, m$) the function was numerically minimized:

$$M = R - \lambda\Omega, \tag{8}$$

where

$$R = \sum_{s=1}^{n}(U(T_s) - V_{INTRA}(T_s))^2;\ \Omega = \sum_{k=1}^{m}(F(r_k)dr_k)^2;$$

and n is the number of experimental points on T. λ is the Tikhonov regularization parameter (21).

The smoothness of the obtained dependence, $F(r)$, depends on the regularity parameter, λ. For small λ values the solution is unstable to little deviations of the experimental V_{INTRA} values, i.e., $F(r)$ may chaotically vary with a large amplitude. At large λ values the solution becomes too smoothed, and consequently characteristic details of the distribution may be lost. Furthermore, it describes the experimental data worse. The optimum was chosen for a value of λ at which a sharp growth of the R value begins.

We employed a range of distances between 1 and 5 nm which was split into equal intervals of 0.25 nm. The obtained distribution function $F(r)$ is illustrated in Fig. 7. The function $U(T)$, obtained from $F(r)$, is shown in Fig. 6.

The distribution function depicted in Fig. 7 exhibits a maximum near 2.5 nm and a half-width of ~1.4 nm. This latter parameter indicates a broad distance distribution. Such a wide distance spectrum could indicate the presence of aggregates of different types.

Effective number of spin labels in aggregates from PELDOR data

According to relationship Eq. 7, the asymptotic value, V_P, is related to the effective number of labels in the aggregates.

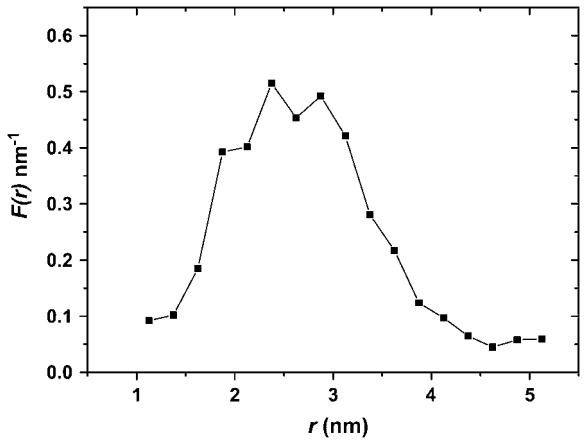

FIGURE 7 Distance distribution function $F(r)$ between spin labels in FTOAC1 aggregates obtained from the data shown in Fig. 6 using the Tikhonov regularization (see text).

From the data in Fig. 6 we obtained $V_P = 0.895 \pm 0.002$. Using this V_P value and the experimental value $p_b = 0.09 \pm 0.01$, we calculate $N = 2.1 \pm 0.1$. Thus, at a (local) peptide concentration of 5 mol % in DPPC membranes, aggregates are mostly formed by pairs of trichogin molecules. It is worth noting that in one of the previous PELDOR studies of spin-labeled trichogin in different membrane-mimicking solvent systems, aggregate numbers were found to vary between $N = 1$ (polar ethanol) and $N = 4.3$ (apolar dichloroethane/toluene) (22). At much lower total concentrations, experiments with fluorescent-labeled trichogin and large unilamellar vesicles (LUVs) of egg phosphatidyl choline (ePC) in the presence of cholesterol showed a lower limit of the number of molecules per aggregate $N = 2.3$ (23). At about the same total concentration, an ion conduction experiment with unlabeled trichogin bound to ePC LUVs in the absence of cholesterol showed that three to four molecules are involved in the rate-limiting step (24). On the other hand, a recent EPR study of trichogin in ePC vesicles showed that at peptide concentrations over the range of 0.5–2.2 mol % monomeric trichogin molecules are homogeneously distributed at the inner and outer membranes (25), whereas upon addition of cholesterol the distribution was found inhomogeneous. Thus, the presence of cholesterol is clearly promoting the formation of thermodynamically stable aggregates. In this EPR study of spin-labeled trichogin in DPPC membranes, however, dimers are formed despite the absence of cholesterol. Since dimers are preferentially formed in rather polar environments (22), it might be plausible that the aggregates observed in DPPC are located at the border between the polar and apolar regions of the membrane. However, we cannot exclude the possibility that, under the conditions used for ion conduction experiments, larger oligomeric species are penetrating the hydrophobic core of the lipid bilayer.

Note also that curve 3 in Fig. 5 has a convex character. Such a behavior significantly differs from the concave dependence $\ln(V) \sim T^{0.75}$, obtained in Milov et al. (14) for similar systems containing a spin-labeled trichogin analog at low concentrations. The convex character of curve 3 in Fig. 5 corresponds to a reduction of the dipole-dipole interactions between the labels responsible for the behavior of V_{INTER} at small T. As these interactions are relatively strong, their reduction suggests a more difficult access to each of the other spin labels from different aggregates due to their relatively large size.

CONCLUSIONS

This ESEEM study of trichogin molecules spin labeled at different positions shows that at low peptide concentration they have an ''in-plane'' orientation with the TOAC4 label near the 9th–11th carbon positions of the *sn-2* side chain of DPPC. Fig. 8 shows the orientation and penetration depth of the peptide with respect to the headgroup and the hydrocarbon core region of the membrane. This model was built by positioning the helical peptide molecule with the amphipathic plane (26) oriented parallel to the surface of the membrane and with the hydrophobic amino acid side chains facing the membrane interior. The thicknesses of headgroup and hydrophobic layers (the levels at 1.1 nm and 3.6 nm are indicated by *dotted* and *solid lines*, respectively) as well as the values of the tilting angles of the fatty acyl chains of the DPPC gel-state were adopted from the literature (27–29). The tilting angle of the *n*-octanoyl side chain of the peptide is assumed to be similar to those of the lipid chains, i.e., 33° away from the bilayer normal. Covalent bond distances of the arbitrarily drawn conformation of the DPPC lipid are the same as those of the peptide. The TOAC4 label is positioned at the same level as that of the 10th carbon atom of the *sn*-2

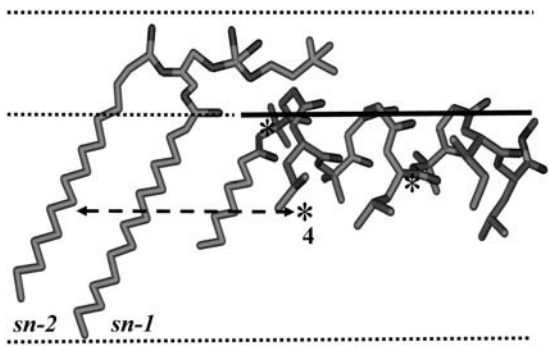

FIGURE 8 Model of the in-plane-bound trichogin GA IV molecule showing its immersion depth in the DPPC gel-state membrane. The 4th TOAC label is located at the same level as that of the 10th carbon atom of the *sn*-2 fatty acyl chain of the lipid (*broken line*). The solid line indicates the amphipathic plane of the peptide molecule separating the opposite hydrophilic and hydrophobic faces of the helix. This plane coincides with the border between the polar interface and the hydrocarbon interior of the membrane. Nitroxide-labeled positions (residues 1, 4, and 8) are depicted by asterisks.

lipid side chain. From this model it appears that the order of the immersion depths shown for different labeled positions of trichogin GA IV is TOAC4 > TOAC8 > TOAC1. The polar face of the amphipathic helix is located at the border separating the interior and interfacial regions of the membrane.

A previous PELDOR study showed that at low concentration, peptide aggregation does not take place (14). However, here we found that upon increasing the peptide concentration, aggregates tend to appear, with a mean number of molecules in the aggregates close to two. The intermolecular distances between the N-terminal residues of their constituent monomers are widely distributed, ranging from 1.5 to 4 nm, suggesting some heterogeneity of the membrane-bound dimer structures. The most abundant dimers exhibit a distance of 2.5 nm, which is of the same order as the length (2.0 nm) of their constituting helical monomers (14). This observation implies the presence of an antiparallel orientation of the two different peptide chains. Assuming that association of the amphipathic molecules leads to dimers with all hydrophobic amino acid side chains oriented to the outside, it is of interest that these ESEEM results showed that the N-terminal residues of the aggregate are located deeper (as compared to the monomer) in the membrane.

The conclusions of this work are in general agreement with those reported by Mazzuca et al. (9). For an ePC bilayer containing 50 mol % of cholesterol and studied at room temperature, these authors found at low P/L ratios, trichogin binds close to the region of polar headgroups. By increasing the concentration up to the level of membrane leakage, a strong correlation was found between the fraction of more deeply buried peptide and the fraction of aggregates (23). Thus, the monomeric and surface-bound peptide molecules are likely biologically inactive, whereas the buried, aggregated peptides are responsible for membrane leakage. The presence of cholesterol in vesicular membranes, however, is questionable if one aims at studying the detailed antibiotic activity of this lipopeptaibol against cholesterol lacking Gram-positive microorganisms. From a previous PELDOR study of trichogin GA IV bound to the cell membrane of *Micrococcus luteus*, it was demonstrated that the peptide molecules are indeed distributed in the cytoplasmic membrane, but aggregates of peptide molecules were not detected (30). As at present no conclusion can be drawn about a possible correlation between membrane leakage and antibiotic activity, we are motivated to continue this research. Nevertheless, for the first time to our knowledge, we have detected formation of dimers upon increasing the concentration of trichogin GA IV in membranes despite the absence of cholesterol.

This work was financially supported by the Russian Grant for Scientific Schools (919.2003.3), the Dutch-Russian Research Cooperation Program (Netherlands Organization of Scientific Research in collaboration with the Russian Foundation of Basic Research) (NWO 047.015.015), and the U.S. Civilian Research & Development Foundation (CRDF) (NO 008-X1 and RUC1-2635-NO-05).

REFERENCES

1. Auvin-Guette, C., S. Rebuffat, Y. Prigent, and B. Bodo. 1992. Trichogin A IV, an 11-residue lipopeptaibol from *Trichoderma longibrachiatum*. *J. Am. Chem. Soc.* 114:2170–2174.
2. Benedetti, E., A. Bavoso, B. Di Blasio, V. Pavone, C. Pedone, C. Toniolo, and G. M. Bonora. 1982. Peptaibol antibiotics: a study on the helical structures of the 2–9 sequence of emerimicins III and IV. *Proc. Natl. Acad. Sci. USA*. 79:7951–7954.
3. Rebuffat, S., C. Goulard, B. Bodo, and M.-F. Roquebert. 1999. The peptaibol antibiotics from *Trichoderma* soil fungi; structural diversity and membrane properties. *Recent Res. Devel. Org. Biorg. Chem.* 3: 65–91.
4. Toniolo, C., M. Crisma, F. Formaggio, C. Peggion, R. F. Epand, and R. M. Epand. 2001. Lipopeptaibols, a novel family of membrane active, antimicrobial peptides. *Cell. Mol. Life Sci.* 58:1179–1188.
5. Peggion, C., F. Formaggio, M. Crisma, R. F. Epand, R. M. Epand, and C. Toniolo. 2003. Trichogin: a paradigm for lipopeptaibols. *J. Pept. Sci.* 9:679–689.
6. Monaco, V., F. Formaggio, M. Crisma, C. Toniolo, P. Hanson, and G. L. Millhauser. 1999. Orientation and immersion depth of a helical lipopeptaibol in membranes using TOAC as an ESR probe. *Biopolymers.* 50:239–253.
7. Epand, R. F., R. M. Epand, V. Monaco, S. Stoia, F. Formaggio, M. Crisma, and C. Toniolo. 1999. The antimicrobial peptide trichogin and its interaction with phospholipid membranes. *Eur. J. Biochem.* 266: 1021–1028.
8. Kaiser, R. D., and E. London. 1998. Determination of the depth of BODIPY probes in model membranes by parallax analysis of fluorescence quenching. *Biochim. Biophys. Acta.* 1375:13–22.
9. Mazzuca, C., L. Stella, M. Venanzi, F. Formaggio, C. Toniolo, and B. Pispisa. 2005. Mechanism of membrane activity of the antibiotic trichogin GA IV: a two-state transition controlled by peptide concentration. *Biophys. J.* 88:3411–3421.
10. Dikanov, S. A., and Yu. D. Tsvetkov. 1992. Electron Spin Echo Envelope Modulation (ESEEM) Spectroscopy. CRC Press, Boca Raton, FL. 1–412.
11. Kurshev, V. V., and L. Kevan. 1995. Electron spin echo modulation studies of doxylstearic acid spin probes in frozen vesicle solutions: interaction of the spin probe with 31P in the surfactant headgroups. *J. Phys. Chem.* 99:10616–10620.
12. Milov, A. D., K. M. Salikhov, and M. D. Shirov. 1981. Application of ELDOR in electron-spin echo for paramagnetic center space distribution in solids. *Fiz. Tverd. Tela.* 23:975–982.
13. Milov, A. D., A. G. Maryasov, and Yu. D. Tsvetkov. 1998. Pulsed electron double resonance (PELDOR) and its application in free radicals research. *Appl. Magn. Reson.* 15:107–143.
14. Milov, A. D., D. A. Erilov, E. S. Salnikov, Yu. D. Tsvetkov, F. Formaggio, C. Toniolo, and J. Raap. 2005. Structure and spatial distribution of the spin-labelled lipopeptide trichogin GA IV in a phospholipid membrane studied by pulsed electron-electron resonance (PELDOR). *Phys. Chem. Chem. Phys.* 7:1794–1799.
15. Toniolo, C., M. Crisma, F. Formaggio, C. Peggion, V. Monaco, C. Goulard, S. Rebuffat, and B. Bodo. 1996. Effect of N^{α}-acyl chain length on the membrane-modifying properties of synthetic analogs of the lipopeptaibol trichogin GA IV. *J. Am. Chem. Soc.* 118:4952–4958.
16. Venanzi, M., E. Gatto, G. Bocchinfuso, A. Palleschi, L. Stella, F. Formaggio, and C. Toniolo. 2006. Dynamics of formation of a helix-turn-helix structure in a membrane active peptide: a time-resolved spectroscopy study. *ChemBioChem.* 7:43–45.
17. Erilov, D. A., R. Bartucci, R. Guzzi, A. A. Shubin, A. G. Maryasov, D. Marsh, S. A. Dzuba, and L. Sportelli. 2005. Water concentration profiles in membranes measured by ESEEM of spin-labeled lipids. *J. Phys. Chem. B.* 109:12003–12013.
18. Toniolo, C., C. Peggion, M. Crisma, F. Formaggio, X. Shui, and D. L. Eggleston. 1994. Structure determination of racemic trichogin A IV using centrosymmetric crystals. *Nat. Struct. Biol.* 1:908–914.

19. Crisma, M., V. Monaco, F. Formaggio, C. Toniolo, C. George, and J. L. Flippen-Anderson. 1997. Crystallographic structure of a helical lipopeptaibol antibiotic analogue. Lett. *Pept. Sci.* 4:213–218.

20. Monaco, V., F. Formaggio, M. Crisma, C. Toniolo, P. Hanson, G. Millhauser, C. George, J. R. Deschamps, and J. L. Flippen-Anderson. 1999. Determining the occurrence of a 3_{10}-helix and an α-helix in two different segments of a lipopeptaibol antibiotic using TOAC, a nitroxide spin-labeled C^{α}-tetrasubstituted α-amino acid. *Bioorg. Med. Chem.* 7:119–131.

21. Chiang, Y.-W., P. P. Borbat, and J. H. Freed. 2005. The determination of pair distance distributions by pulsed ESR using Tikhonov regularization. *J. Magn. Reson.* 172:279–295.

22. Milov, A. D., Yu. D. Tsvetkov, and J. Raap. 2000. Aggregation of trichogin analogs in weakly polar solvents: PELDOR and ESR studies. *Appl. Magn. Reson.* 19:215–226.

23. Stella, L., C. Mazzuca, M. Venanzi, A. Palleschi, M. Didonè, F. Formaggio, C. Toniolo, and B. Pispisa. 2004. Aggregation and water membrane partition as major determinants of the activity of the antibiotic peptide trichogin GA IV. *Biophys. J.* 86:936–945.

24. Kropacheva, T. N., and J. Raap. 2002. Ion transport across a phospholipid membrane mediated by the peptide trichogin GA IV. *Biochim. Biophys. Acta.* 1567:193–203.

25. Milov, A. D., R. I. Samoilova, Yu. D. Tsvetkov, F. Formaggio, C. Toniolo, and J. Raap. 2005. Membrane-peptide interaction studied by PELDOR and cwEPR. Peptide conformations and cholesterol effect on the spatial peptide distribution in the membrane. *Appl. Magn. Reson.* 29:703–716.

26. Kropacheva, T. N., E. S. Salnikov, H.-H. Nguyen, S. Reissmann, Z. A. Yakimenko, A. A. Tagaev, T. V. Ovchinnikova, and J. Raap. 2005. Membrane association and activity of 15/16 peptide antibiotics: zervamicin IIB, ampullosporin A and antiamoebin I. *Biochim. Biophys. Acta.* 1715:6–18.

27. Marsh, D. 1990. Handbook of Lipid Bilayers. CRC Press, Boca Raton, FL.

28. Lewis, B. A., and D. M. Engelman. 1983. Lipid bilayer thickness varies linearly with acyl chain length in fluid phosphatididylcholine vesicles. *J. Mol. Biol.* 166:211–217.

29. Rinia, H. A., R. A. Kik, R. A. Demel, M. M. E. Snel, J. A. Killian, J. P. J. M. van der Eerden, and B. de Kruijff. 2000. Visualization of highly ordered striated domains induced by transmembrane peptides in supported phosphatidylcholine bilayers. *Biochemistry.* 39:5852–5858.

30. Milov, A. D., R. I. Samoilova, Yu. D. Tsvetkov, V. A. Gusev, F. Formaggio, M. Crisma, C. Toniolo, and J. Raap. 2002. Spatial distribution of spin-labeled trichogin GA IV in the Gram-positive bacterial cell membrane determined from PELDOR data. *Appl. Magn. Reson.* 23:81–95.